Effect of film thickness on the structural morphological and optical properties of nanocrystalline ZnO films formed by RF magnetron sputtering

R. Subba Reddy[1*], A. Sreedhar[1], A. Sivasankar Reddy[2], S. Uthanna[1*]

[1]Department of Physics, Sri Venkateswara University, Tirupati 517 502, India
[2]Division of Advanced Materials Engineering, Kongju National University, Budaedong, Cheonan city, South Korea

[*]Corresponding authors. Tel: (+91) 9440650393; E-mail*: sbbreddy82@gmail.com (R.S. Reddy), uthanna@rediffmail.com (S. Uthanna).

ABSTRACT

Zinc oxide (ZnO) thin films were formed by RF reactive magnetron sputtering onto p-type silicon and glass substrates held at room temperature. The thickness of the films deposited was in the range 160 – 398 nm. The thickness dependence structural, morphological and optical properties of ZnO films were systematically investigated. The maximum crystallite size of 21 nm observed at films thickness of 231 nm by X- ray diffraction. Scanning electron microscopic analysis revealed that the growth of nanowires in all the films. The root mean square roughness of the films increased from 7.3 to 53 nm in the thickness range of investigation. Fourier transform infrared analysis confirmed the Zn-O bonding located at wavenumber of 413 cm^{-1}. The average optical transmittance of the films was about 89 % in the visible region. The optical band gap of the ZnO films decreased from 3.14 to 3.02 eV with increase of film thickness from 160 to 398 nm respectively. Copyright © 2012 VBRI Press.

Keywords: Thin films; sputtering; ZnO films; structure; optical properties.

R. Subba Reddy is presently research scholar under the guidance of Prof S. Uthanna, Dept. Physics, Sri Venkateswara University, Tirupati, India. Currently he is working on the RF magnetron sputtered ZnO films. He received his Master Degree in Physics from the Sri Krishnadevaraya University, Anantapur, India during the year 2005-07.

A. Sreedhar received his Master Degree in Physics from Sri Krishnadevaraya University, Anantapur, India during 2006-2008. Present he is research scholar in the Department of Physics, Sri Venkateswara University, Tirupati, India. He is working on pure and doped copper oxide thin films for transparent conductor applications.

A. Sivasankar Reddy is working as a postdoctoral fellow, Green Home Energy Technology Research center, Kongju National University, South Korea. He obtained Ph.D. from the Department of Physics, Sri Venkateswara University, Tirupati, India, under the supervision of Prof. P. Sreedhara Reddy and, with co-guidance of Prof. S. Uthanna, in 2006. He has worked as a postdoctoral fellow in the Department of Materials Science and Engineering, Yonesi University,

South Korea in 2006-08, and SEG-CEMUC- Department of Mechanical Engineering, University of Coimbra, Portugal in 2008-2010. He has published more than 35 papers in the reputed International Journals.

Suda Uthanna (born in 1955) received his Ph. D degree in Physics in 1983 from Sri Venkateswara University. He is Professor since 2004 in the Department of Physics, Sri Venkateswara University, Tirupati, India. He is actively engaged in the research work in semiconducting and oxide thin films for energy conversion and microelectronic devices. He was International Union for Vacuum Science and Technology Applications WELCH fellow in 1989. He has published over 160 papers in the International and National Journals.

Introduction

Zinc Oxide (ZnO) is an attractive semiconducting material due to its promising properties of high electrical conductivity and good optical transparency. It has advantages of nontoxicity, low cast and abundance of raw material with high stability [1]. ZnO was found various technological applications such as solar cells [2], active material for highly sensitive humidity and oxygen gas sensors [3, 4], transparent electrodes for flat –panel displays [4], p-n junction diodes [5], UV photodetectors [6], ultraviolet light emitting diodes [7], transparent thin film transistors [8] and piezoelectric nanogenerators [9]. In the recent years, the novel ZnO nanostructures are reported to have potential applications for optical emission, catalysis, sensing, actuation, and drug delivery [10]. The increase in surface area and the quantum confinement effects have made nanostructured materials are quite distinct from their bulk form in both electrical and optical properties. Various one-dimensional structures of ZnO, such as nanowires, nanorods, and nanobelts, have attracted much attention [11, 12]. ZnO thin films have been grown by various deposition techniques such as thermal oxidation of zinc [13], chemical bath deposition [14], spray pyrolysis [15, 16], sol-gel process [17], electron beam evaporation [18], atomic layer deposition [19], pulsed laser deposition [20], metal organic chemical vapor deposition [21], molecular beam epitaxy [22, 23], and DC [24-28] and RF [29-33] magnetron sputtering and electrodeposition [34]. The physical properties of the formed films depend on the deposition method employed and process parameters maintained during the growth of the films. Among these deposition techniques, magnetron sputtering is industrially adopted thin films preparation method because of the advantages in the generation of uniform and large area films. The physical properties of the sputtering films depends mainly on the process parameters such as oxygen partial pressure, sputter power, substrate temperature, substrate bias, thickness and post deposition annealing. Wang et al. [35] observed that the ZnO films formed by RF magnetron sputtering at low oxygen flow rate of 2 sccm the surface in the shape of rods with diameter about 200 nm and the rods separated with the large distance of 0.3 – 2.0 µm. The average surface roughness of the films decreased to 0.42 nm with increase of oxygen flow rate of 6 sccm. The films formed were polycrystalline with wurtzite structured ZnO and the intensity of (002) orientation increased with increase of oxygen flow rate due to decrease of oxygen vacancies. The optical band gap of the films increased from 3.10 to 3.24 eV with increase of oxygen flow rate from 0 to 6 sccm. Mandal et al. [36] achieved wurtzite structured ZnO films with increase in grain size from 30 to 50 nm and root mean square surface roughness increased from 8 to 12 nm and the band gap decreased from 3.32 to 3.24 eV with increase of substrate temperature from 313 to 673 K. Daniel et al. [31] reported that the crystallite size of the films increased from 16 to 27 nm and optical band gap decreased from 3.29 to 3.25 eV in the as-deposited and the films annealed at 673 K respectively. Hoon et al. [28] reported that the grain size of the films increased from 137 to 230 nm and surface roughness of the films increased from 2.3 to 8.0 nm with increase of films

thickness from 150 to 700 nm in DC magnetron sputtered ZnO films. Thin films exhibited high optical transmittance in the range 70 – 90 %. The transmittance decreased to 50-70% in the wavelength range 400 - 850 nm, when the deposited film thickness beyond the 700 nm. In the present investigation, ZnO films with various thicknesses in the range 160-398 nm by using RF magnetron sputtering techniques. The effect of film thickness on the structural, morphological and optical properties of ZnO films was systematically studied and reported the results.

Experimental

Thin films of zinc oxide were formed on to well cleaned p-silicon (100) and Corning glass substrates held at room temperature by RF magnetron sputtering method. Metallic zinc target (99.99 % pure supplied by Nuclear Fuel Complex, India) with 50 mm diameter was used as sputter target for deposition of experimental films in the sputter up configuration. The sputter chamber was evacuated to the base pressure of $2x10^{-4}$ Pa employing diffusion pump and rotary pump combination along with liquid nitrogen trap. Pressure in the sputter chamber was measured with digital Pirani - Penning gauge combination. Argon and oxygen (99.999 % purity) were used as sputter and reactive gases for deposition of the films. Individual Aaloborg (Model GFC 17) mass flow controllers were employed to admit these gases in required quantities in the sputter chamber. After attaining the ultimate base pressure of $2x10^{-4}$ Pa, oxygen gas was introduced to the pressure of $2x10^{-2}$ Pa. Later argon gas was admitted to achieve sputter pressure of 5 Pa. Radio frequency (RF) power (Advanced Energy Model ATX-600 W) fed to the sputter target was 150 W. ZnO films with different thicknesses were deposited by varying the deposition times. The deposition conditions maintained during the growth of the ZnO films are given in **Table 1**.

Table 1. Deposition parameters for the growth of ZnO films.

Sputter target	:	Zn
Target to substrate distance	:	50mm
Base pressure	:	$2x10^{-4}$ Pa
Oxygen partial pressure (pO₂)	:	$2x10^{-2}$ Pa
Sputter pressure	:	5 Pa
Sputter power	:	150 W
Film thickness	:	160 - 398 nm

The thickness of the deposited films was measured using Vecco Dektak (Model 150) depth profilometer. The crystallographic structure of the films was determined with glancing angle X- ray diffractometer (Bruker D8 Advance diffractometer) at the glancing angle of 4° with monochromatic Co $K_{\alpha1}$ radiation with wavelength of 1.7889 A^o. The surface morphology of the films was analysed with scanning electron microscope (Hitachi SEM Model S: 4000) and atomic force microscope (Bench Apparatus digital Instrument Model 3100). Fourier

transform infrared spectrophotometer (Nicolet Magana IR 750) was used to record the transmittance in the wavenumber in the range 400 - 4000 cm^{-1}. The optical transmittance of the films was recorded using UV-Vis-NIR double beam spectrophotometer (Perkin – Elmer Lambda 950) in the wavelength range 300 -1200 cm.
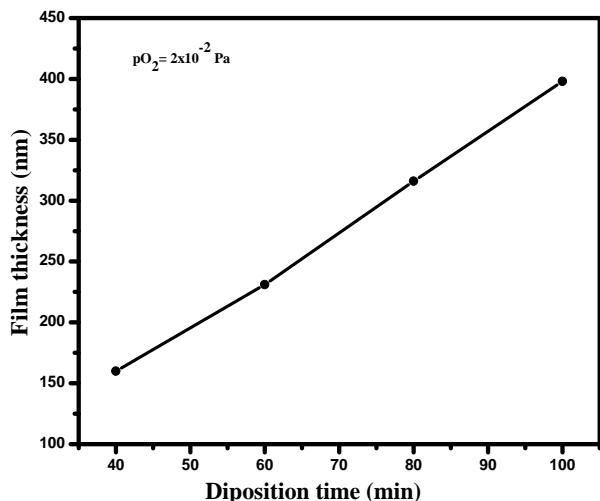
Fig. 1. Dependence of ZnO film thickness on the deposition time.
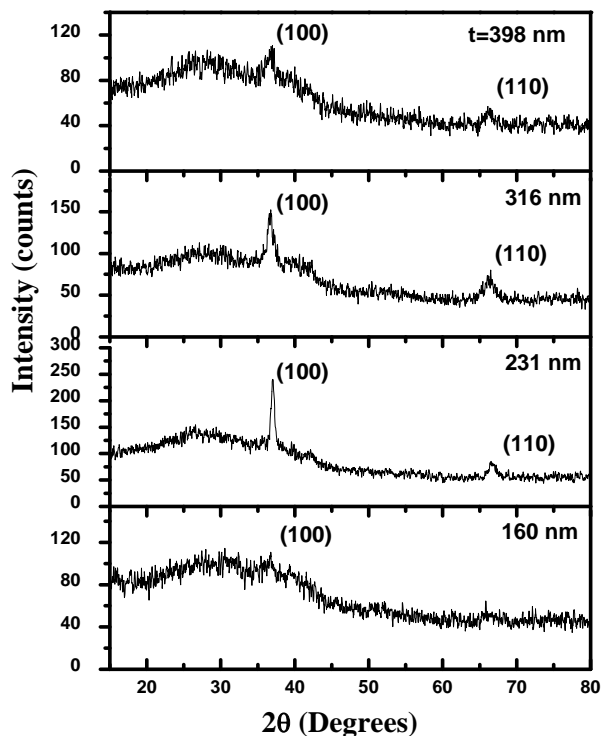
Fig. 2. XRD profiles of ZnO films of different thicknesses.

Results and discussion

Film thickness is one of the crucial factors for application of transparent films. ZnO films with different thicknesses were deposited by varying the time of deposition by fixing other deposition parameters as constant. The thickness of the deposited films determined with depth profilometer was increased from 160 to 398 nm with the increase of deposition time from 40 to 100 minutes. **Fig. 1** shows the dependence of film thickness on the deposition time. The thickness of the films increased nearly linearly with the increase of deposition time. The deposition rate of the films determined from the film thickness and the deposition time was about 3.91 nm/min. Thin films formed at less deposition times were low thickness and contributes to higher transparency and reduction in the electrical resistivity.
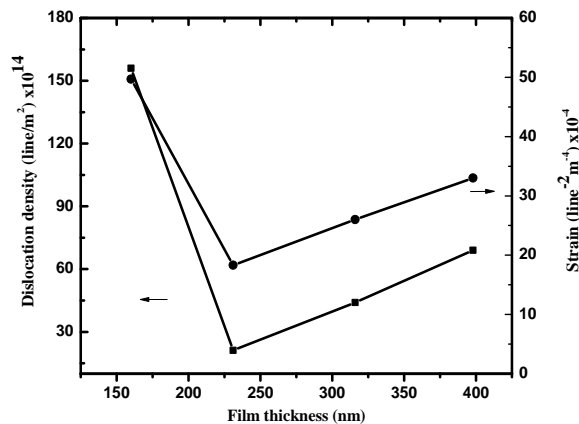
Fig. 3. Dependence of dislocation density and strain on thickness of the ZnO films.

Structural analysis

Fig. 2 shows the X-ray diffraction profiles of ZnO films in the thickness of 160, 231, 316 and 398 nm. From the XRD profile, the films deposited at thickness of 160 nm exhibited the (100) orientation at $2\theta = 37.1^0$ with less intensity indicated that the nanocrystals were embedded in amorphous matrix. As the film thickness increased to 231 nm, the intensity of the (100) was increased greatly and an additional peak was located at 66.6^0 related to the (110) orientation indicated that the films were nanocrystalline in nature [JCPDS card no: 89 - 1397]. Further increase of thickness to 316 nm the intensity of the diffraction peaks decreased. At higher thickness of 398 nm the intensity of (100) and (110) reflections diminished revealed the reduction in the crystallinity of the films. In the literature, Bouderbala et al. **[29]** also achieved amorphous films at low thickness of 70 nm in RF magnetron sputtered ZnO films. The peak intensity and crystallinity are associated with the crystallinity of the deposited films. According to the crystal growth mechanism the growth faces of crystallites correspond to the crystal shape of equilibrium determined by the orientation of the crystal **[22]**. The dislocation density (δ) and the strain (ε) developed in the films were calculated from the X-ray diffraction (100) reflection using the relation **[37]**.

$$\delta = 1/L^2 \qquad\qquad (1)$$
$$\varepsilon = \beta\cos\theta/4 \qquad\qquad (2)$$

where β is the full width at half maximum (FWHM) intensity. **Fig. 3** shows the dependence of dislocation

density and strain developed on the thickness of the films. The dislocation density of the ZnO films decreased from 1.57×10^{16} to 1.8×10^{15} lines/m^2 with increase of film thickness from 160 to 231 nm, there after increased to 6.5×10^{15} lines/ m^2 at higher thickness of 398 nm. The strain in the films first decreased from 5×10^{-3} line^{-2} /m^4 to 1.8×10^{-3} line^{-2} /m^4 with increase of film thickness from 160 to 231 nm due to the transformation from amorphous to nanocrystalline.

A gradual increase in the strain to 3.3×10^{-3} line^{-2} /m^4 at higher thickness of 398 nm was due to the decrease in the crystallinity of the films. The crystallite size (L) of the films was calculated from the (100) reflection peak using the Debye- Scherrer's relation [38]

$$L = 0.9\lambda/\beta\cos\theta \qquad (3)$$
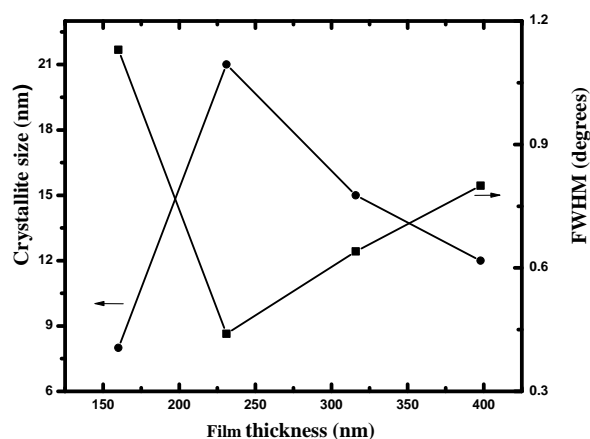
Fig. 4. Variation of crystallite size and FWHM with thickness of the ZnO films.
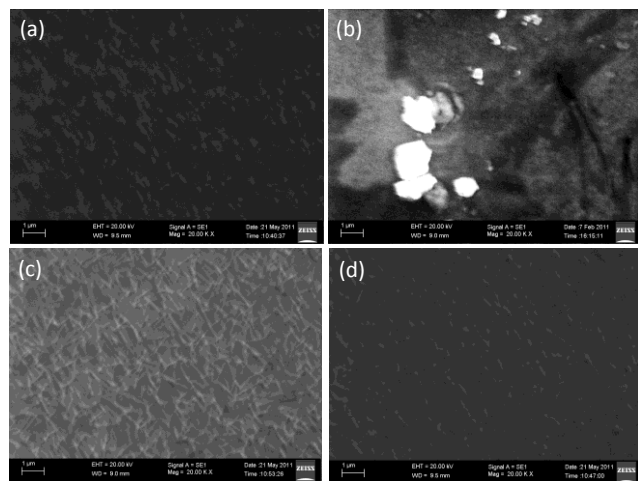
Fig. 5. Scanning electron micrographs of ZnO films of different thicknesses: (a) 160 nm, (b) 231 nm, (c) 316nm and (d) 398 nm.

Fig. 4 shows the variation of full width at half maximum and crystallite size with the thickness of ZnO films. The full width at half maximum intensity decreased from 1.13 to 0.44^0 with the increase of film thickness from 160 to 231 nm, thereafter it increased to 0.81^0 at higher thickness of 398 nm. The crystallite size of the films increased from 8 to 21 nm with increase of film thickness

from 160 to 231 nm while at higher thickness of 398 nm it was decreased to 12 nm. At low thickness of 160 nm the high value of full width at half maximum and small crystallite size of 8 nm was due to the amorphous nature of the films. It is in accordance with the report on RF magnetron sputtered ZnO films where the amorphous nature observed at thickness of 70 nm [29]. As the thickness increased to 231 nm the crystallinity of the films improved this indicated the nanocrystalline films, hence decrease in the full width at half maximum to 0.44 there by enhancement in the crystallite size to 21 nm. At higher thickness the increase in full width at half maximum and decrease in the crystallite size was due to the reduction in the crystallinity of the films.

(a) RMS = 7. 3 nm

(b) RMS = 40 nm

(c) RMS = 53 nm
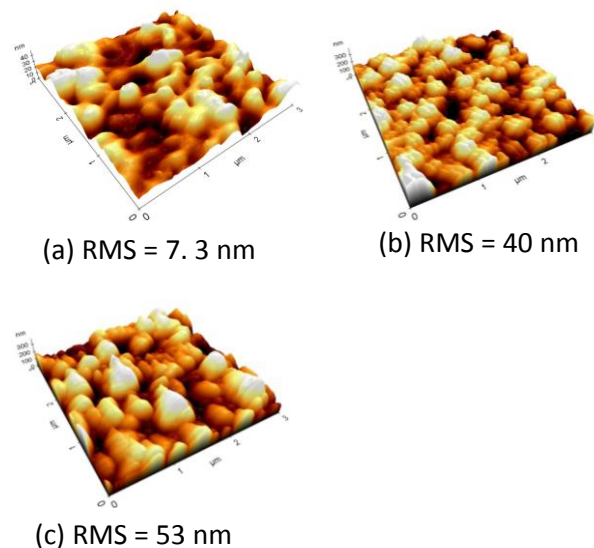
Fig. 6. Atomic force micrographs of ZnO films of different thicknesses: (a) 231 nm, (b) 316 nm and (c) 398 nm.

SEM analysis

Fig. 5 shows the SEM images of ZnO films of different thicknesses. It is seen from the figures that thin films of 160 nm exhibited smaller size nanowires. When the thickness of the films increased to 231 nm, the shape of nanowires disappeared and presence of dense surface with porous like structure due to improvement in the crystallinity of the films. It was also supported by the XRD analysis that the crystallinity enhanced as the thickness of the films increased to 231 nm. Further increase of film thickness to 316 nm, the dense surface structure disappeared and growth of nanowires with length of about 450 nm. Further increase of film thickness to 398 nm the number and size of nanowires were decreased due to reduction in the crystallinity [20, 23].

AFM analysis

Fig. 6 shows the atomic force morphological images of ZnO films formed at different thicknesses. The atomic force microscopy was used to determine average size of the grains nucleated in the ZnO films. For the film thickness of 231 nm the root mean square roughness (RMS) was 7.3 nm. With increase of film thickness to 398 nm the RMS

roughness is gradually increased to 53 nm. The increase of RMS roughness with the increase of film thickness was due to the larger size grains formation as well as increase in the porosity of the films [39]. Such an increase of film thickness was also noticed by Hoon et al. [28]. The increase of RMS roughness of ZnO films leads significant effect on the industrial applications such as gas sensors.
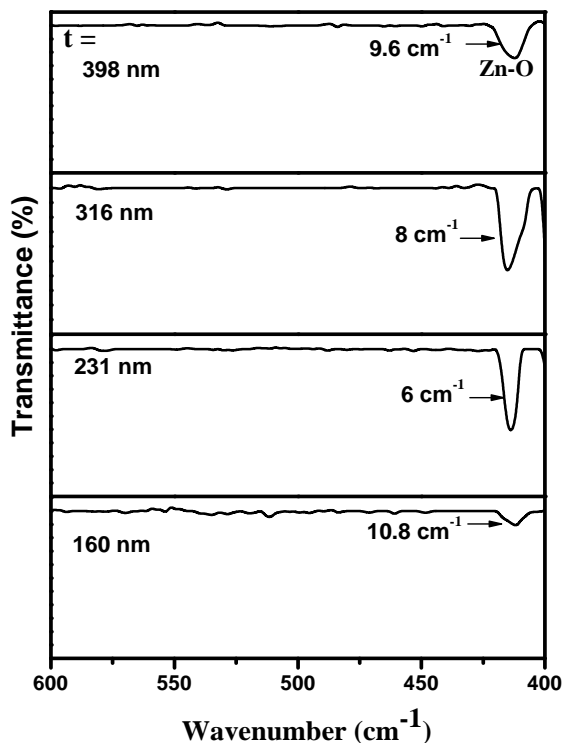
Fig. 7. Fourier transform infrared transmittance spectra of ZnO films.
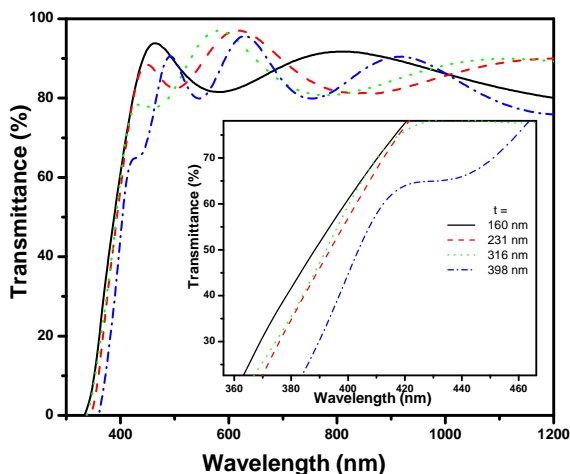
Fig. 8. Optical transmittance spectra of ZnO films of different thicknesses.

FTIR analysis

Fig. 7 shows the FTIR transmittance spectra recorded on the ZnO films formed on p-silicon substrates of different film thicknesses. An absorption band observed at 412 cm^{-1} corresponds to the Zn-O stretching vibration of hexagonal ZnO [27]. The film deposited at low thickness of 160 nm contained the full width at half maximum was 10.8 cm^{-1}. As

the film thickness of the films increased to 231 nm, the FWHM of the absorption band decreased to 6 cm^{-1} due to improvement in the crystallinity as supported the XRD data. Further increase of the film thickness to 398 nm the FWHM increased to 9.6 cm^{-1} due to decrease of (100) phase intensity and degradation of crystallinity.
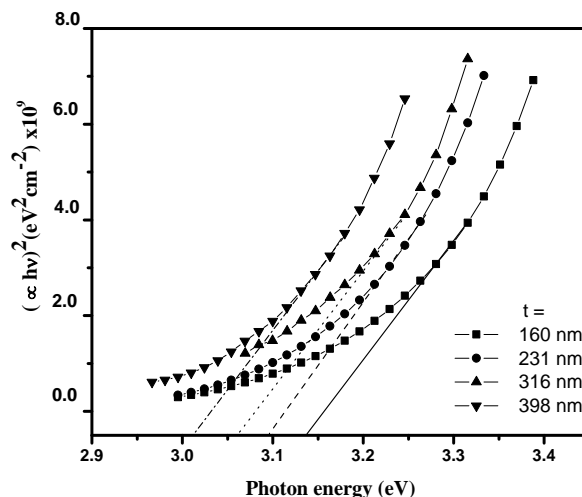
Fig. 9. Plot of $(\alpha h\nu)^2$ versus photon energy (hν) of ZnO films.

Optical properties

Optical transmittance data gives the information on the energy band gap, extinction coefficient and refractive index of the deposited films. **Fig. 8** displays the optical transmittance spectra of ZnO films of different thicknesses. The optical transmittance of ZnO films increased with increase of the films thickness upto 231 nm and then decreased at higher thickness of 398 nm. The average optical transmittance was 89 % in the visible wavelength range 450 - 650 nm. Sharp absorption edge was observed at the wavelength of about 405 nm and shifted towards higher wavelengths side with increase of films thickness in the thickness range of investigation. The optical absorption coefficient (α) was calculated from the film thickness and optical transmittance data using the relation

$$\alpha = (1/t)\ln T \qquad (4)$$

The optical band gap (E$_g$) of the ZnO films can be calculated from the relation [16]

$$(\alpha h\nu) = A(h\nu - E_g)^{1/2} \qquad (5)$$

where A is the edge width parameter and hν the incident photon energy.

Fig. 9 shows the plots of $(\alpha h\nu)^2$ versus photon energy of ZnO films. The optical band gap of ZnO films decreased from 3.14 to 3.02 eV with the increase of films thickness from 160 to 398 nm. The decrease in the optical band gap with the increase of film thickness was due to decrease of lattice defects [40]. The extinction coefficient (k) of the films was also calculated by using the relation

$$k = \alpha\lambda/4\pi \qquad (6)$$

The extinction coefficient of the ZnO films first increased from 1.5 to 2.3 with increase of film thickness from 160 to 231 nm and thereafter decreased to 0.54 at high thickness of 398 nm (**Fig. 10**). The refractive index (n) of the films was determined from the optical transmittance interference data employing Swanepoel's envelope method from the relation **[41]**

$$n(\lambda) = [N + (N^2 - n_0^2 n_1^2)^{1/2}]^{1/2} \qquad (7)$$

$$N = 2n_0 n_1 [(T_M - T_m)/T_M T_m] + [(n_0^2 + n_1^2)/2] \qquad (8)$$

where T_M and T_m are the optical transmittance maxima and minima and n_0 and n_1 the refractive indices of air and substrate respectively. The variation of refractive index and extinction coefficient (at 500 nm) of the films as a function of film thickness are shown in **Fig. 10.**
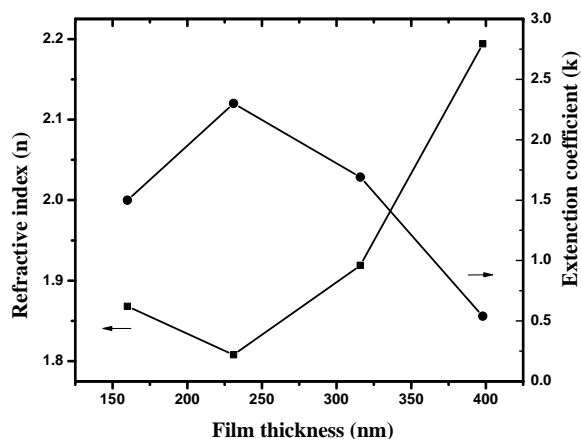
Fig. 10. Dependence of refractive index and extinction coefficient on thickness of ZnO films.

The refractive index of ZnO films first decreased from 1.86 to 1.80 with increase of film thickness from 160 to 231 nm, thereafter the refractive index increased to 2.19 with increase of film thickness to 398 nm as shown in the **Table 2**.

Film thickness (nm)	FWHM (degree)	Crystallite size (nm)	Optical band gap (eV)	Refractive index
160	1.13	8	3.14	1.86
231	0.44	21	3.10	1.80
318	0.64	15	3.06	1.91
398	0.80	12	3.02	2.19

Conclusion

The film thickness dependence of structural, morphological and optical properties of nanocrystalline hexagonal ZnO films deposited by RF magnetron sputtering on glass and silicon p-type (100) substrates held at room temperature was systematically studied. The XRD analysis revealed that low value of FWHM of 0.44^0 and maximum crystallite size of 21 nm was found at film thickness of 231 nm. The FTIR spectrum revealed the Zn-O bonding confirmed at

wavenumber of about 413 cm^{-1}. The SEM images revealed the nanowires with length of about 450 nm at films thickness of 318 nm. The optical studies revealed the maximum transmittance of 96 % found in film thickness of 231 nm. The optical band gap of ZnO films decreased from 3.14 to 3.02 eV with increase of film thickness from 160 to 398 nm.

Reference

1. Wang, ZL. J. Phys.: *Condens. Mater*. **2004**, *16*, 829.
   DOI: 10.1088/0953-8984/16/25/R01
2. Jeong, W.J.; Kim, SK.; Park, SC. *Thin Solid Films*. **2006**, *506-507*, 180.
   DOI: 10.1016/j.tsf.2005.08.21
3. Chen, Z.; Lu, C. Sens. Lett. **2005**, *3*, 274.
   DOI: 10.1166/sl.2005.045
4. Jeong, MC.; Oh, BY.; Nam, OW.; Kim,T.; Myoung, JM. *Nanotechnology*. **2006**, *17*, 526.
   DOI: 10.1088/0957-4484/17/2/031
5. Kumar, M.; Prakash Kar, J.; Kim, IS.; Choi, SY.; Myoung, JM. *Curr. Appl. Phys*. **2011**, 11, 65.
   DOI: 10/1066/j.cap.2010.06.020
6. Look, DC. *Mater. Sci. B*. **2001**, *80*, 383.
   DOI: S0921-5107(00)00604-8
7. Ryu, Y.; Lee, TS.; Jorge, AL.; White, HW.; Kim, BJ.; Park, YS.; Youn, CJ. *Appl. Phys. Lett*. **2006**, *88*, 241108.
   DOI: 10.1063/1.2210452
8. Carcia, PF.; McLean, MH.; Reilly, MH.; Nunes, G. *Appl. Phys. Lett*. **2006**, *82*, 1117.
   DOI: 10.1063/1.1553997
9. Wang, ZL.; Song, J. *Science* **2006**, *312*, 243.
   DOI: 10.1126/science.1124005
10. Tian, ZR.; Voigt, JA.; Liu, J.; Mckenzie, B.; Mc Dermott, MJ.; Rodriguez, MA.; Kingishi, H.; Xu, H. *Nat. Mater*. **2003**, *2*, 821.
    DOI: 10.1038/nmat1014
11. Roy, VAL.; Djurisic, AB.; Chan, WK.; Gao, J.; Lui, HF.; Surya, C. *Appl. Phys. Lett*. **2003**, *83*, 141.
    DOI: 10.1063/1.1589184
12. Han, J.; Zhu, Z.; Ray, S.; Azad, AK.; Zhang, W.; He, M.; Li, S.; Zhao, Y. *Appl. Phys. Lett*. **2006***, 89*, 031107.
    DOI: 10.1063/1.2222329
13. Xu, CH.; Lui, HF.; Surya, C. *Mater. Lett*. **2011**, *65*, 27.
    DOI: 10.1016/j.matlet.2010.09.052
14. Ouerfelli, J.; Regragui, M.; Morsli, M.; Djeteli, G.; Jondo, K.; Amory, C.; Tehangbedg, G.; Napo. K.; Berede, JC. *J. Phys. D: Appl. Phys*. **2006**, *39*, 1954.
    DOI: 10.1088/0022-3727/39/9/035
15. Tarwal, NL.; Patil, PS. *Appl. Surf. Sci*. **2010**, *256*, 7451.
    DOI: 10.1016/j.apsusc.2010.05.089
16. Thilakan, P.; Redheep, DM.; Saravana Kumar, K.; Sasikala, G. *Semicond. Sci. Technol*. **2009**, *24*, 085020.
    DOI: 10.1088/0268-1242/24/8/085020
17. Suwanboon, S.; Tanattha, R.; Tanakorn, R. *Songklanakarin J. Sci. Technol*. **2008**, *30*, 65.
    DOI: 10.1016/1025-21/105/024512
18. Mahmood, A.; Ahmed, N.; Raza, Q.; Khan, TM.; Mehmood, M.; Hassan, MM.; Mahmood, N. *Phys. Scripta*. **2010**, *82*, 065801.
    DOI: 10.1088/0031-8949/82/06/065801
19. Pong, SY.; Choy, KL.; Hou, X.; Shan, C. *Nanotechnology*. **2008**, *19*, 435609.
    DOI: 10.1088/0957-4484/19/43/435609
20. Nakamura, D.; Okazaki, K.; Palani, IA.; Higashihata, M.; Okada, T. *Appl. Phys. A*. **2011**, *103*, 959.
    DOI: 10.1007/s00339-011-6401-5
21. Kong, BH.; Kim, DC.; Mohanta, SK.; Cho, HK. *Thin Solid Films.* **2010**, *518*, 2975.
    DOI: 10.1016/j.tsf.2009.10.124
22. Knuyt, G.; Quaeyhaegens, C.; Haen, JD.; Stals, LM. *Phys . Stat. Solidi B*. **1996**, *195*, 179.
    DOI: 10.1016/j.pss.1996.08.005
23. Wu, CC.; Wuu, DS.; Lin, PR.; Chen, TN.; Horng, RH. *Nanoscale Res. Lett*. **2009**, *4*, 377.
    DOI: 10-1007/s11671-009-9257-2

24. Uthanna, S.; Subramanyam, TK.; Srinivasulu Naidu, B.; Mohan Rao, G. *Opt. Mater.* **2002**, *19*, 461.
   DOI: PII: SO925-3467(02)00028-9
25. Martins, R.; Igreja. R.; Ferreira. I.; Marques, A.; Pimentel. A, ; Goncalves. A.;   Fortunato, E. *Mater. Sci. Eng B.* **2005**, *18*, 135.
   DOI: 10.1016/j.msed.2004.12.089
26. Minami, T.; Oda, J.; Nomoto, J.; Miyata,T. *Thin Solid Films*. **2010**, *519*, 385.
   DOI: 10.1016/j.tsf.2010.08.007
27. Kannan, PK.; Saraswathi, R.; Balaguru Rayappan, JB. *Sensors and Actuators A*. **2010**, *164*, 8.
   DOI: 10.1016/j.sna.2010.09.006
28. Hoon, JW.; Chan, KY.; Krishnasamy, J.; Tou, TY.; Knipp, D . *Appl. Surf. Sci*. **2011**, *257*, 2508.
   DOI: 10.1016/j.apsusc.2010.10.012
29. Bouderbala, M.; Hamzaoui, S.; Amrani, B.; Reshak, AH.; Adnane, M.; Sahraoui, T.; Zerdali, M. *Physica B.* **2008**, *403*, 3326.
   DOI:10.1016/j.physb.2008.04.045
30. Li, C.; Matsuda, T.; Kawaharamura, T.; Furuta, H.; Furuta, M.; Hiramatsu, T.; Hirao, T.; Nakamishi, Y.; Ichinomiya, K, *J. Vac. Sci. Technol B*. **2010**, *28*, C2B51.
   DOI: 10.1116/1.3271250
31. Daniel, GP.; Justin Victor, VB.; Nair, PB.; Joy, K.; Koshy, P.; Thomas, PV. *Physica B.* **2010**, *405*, 1782.
   DOI: 10.1016/ j.physb.2010.09.039
32. Kumar, M.; Prakash Kar, J.; Kim, IS.; Choi, SY.; Myoung, JM. *Curr. Appl. Phys.* **2011**, *11*, 65.
   DOI: 10.1016/j.cap.2010.06.020
33. Liu, C.; Morkoc, H. *Superlatt. Microstruc* . **2010**, *48*, 502.
   DOI: 10.1016/j.spmi.2010.09.002
34. Kamal Singh, N.; Shrivastava, S.; Rath, A.; Annapoorna, S. *Appl. Surf. Sci.* **2010**, *257*, 1544.
   DOI: 10.1016/j.apsusc.2010.08.093
35. Wang, XC.; Chen, XM.; Yang, BH. *J. Alloys. Comp*. **2009**, *488*, 232.
   DOI: 10.1016/j.jallcom.2009.08.089
36. Mandal, S.; Singh, PK.; Dhar, A.; Ray, SK. *Mater. Res. Bull*. **2008**, *43*, 244.
   DOI: 10.1016/j.materresbull.2007.05.006
37. Lalitha, S.; Sathyamurthy, R.; Senthilarasu, S.; Subbarayan, A.; Natarajan, K. *Solar Energy Mater. Solar Cells*. **2004**, *82*, 187.
   DOI: 10.1016/j.solmat.2004.01.017
38. Cullity, BD. *Elements of X-ray Diffraction, IInd Ed, Addison Wesley, London.* **1978**.
   DOI: 10.1107/S0567739479000917
39. Kakani, N.; Jee, SH.; Kim, SH.; Oh, JY.; Yoon, YS. *Thin Solid Films.* **2010**, *519*, 494.
   DOI: 10.1016/j.tsf.2010.08.005
40. Lin, YC.; Wang, BL.; Yen, WT.; Ha, CT.; Peng, C. *Thin Solid Films.* **2010**, *518*, 4928.
   DOI: 10.1016/j.tsf.2010.03.007
41. Swanepoel, RJ. J. Phys. E: Sci. Instru. **1983**, *16*, 1214.
   DOI: 10.1007/s00339-010-5632-1